ANALYZING THE EFFECTS OF BODY SIZE ON FROG SWIMMING

By

JACK SPICER

Bachelor of Science in Integrative Biology

Oklahoma State University

Stillwater, OK

2018

Submitted to the Faculty of the
Graduate College of the
Oklahoma State University
in partial fulfillment of
the requirements for
the Degree of
MASTER OF SCIENCE
July, 2021

ANALYZING THE EFFECTS OF BODY SIZE ON

FROG SWIMMING

Thesis Approved:

Thesis Adviser's Name Here

Dr. Daniel Moen

Thesis Adviser

Dr. Arvind Santhanakrishnan

Dr. Haley O'Brien

I would like to acknowledge the following people for their contributions, and continued support

Dr. Gen Morinaga
Dr. Vishwa Kasoju
Dr. Manikantam Gaddam
Mitchell Ford

Name: JACK SPICER

Date of Degree: JULY 2021

Title of Study: ANALYZING THE EFFECTS OF BODY SIZE ON FROG SWIMMING

Major Field: INTEGRATIVE BIOLOGY

Abstract: The scaling of traits with body size, along with the effects it has on performance and evolution, has long been studied in evolutionary biology and biomechanics. These effects can be observed in locomotion across many different organisms. Understanding exactly how characteristics of locomotor performance scale with body size, as well as how body size might constrain performance, are keys for understanding how body size affects performance and evolution. In this study I quantified swimming performance across a range of body sizes (snout vent length, SVL) in the semi-aquatic frog species *Rana catesbeiana*. First, I defined swimming performance as peak swimming speed, due to its importance in the survival of *Rana catesbeiana.* Next, I identified and quantified factors that should affect velocity as well as scale with body size (drag, peak momentum, and wake circulation). Using high-speed recordings of swimming trials paired with digital particle image velocimetry (PIV), I extracted both the swimming speed and the resulting flow velocity. Velocity vector fields from PIV analysis allowed me to quantify momentum and circulation of the flow. Drag force data were acquired by towing specimens on a linear actuator fitted with a strain gauge. To summarize the effect of body size on swimming speed and these performance variables, I fit ordinary least squares regressions between SVL and the variables of swimming speed, momentum, and circulation. My analysis showed that SVL had no significant effect on swimming speed, momentum, or circulation. Drag force profiles showed that larger animals do experience higher resistive drag force at higher speeds, consistent with expectations. The lack of effect of body size on performance variables could have resulted from study limitations, such as small sample size and sub-optimal performance data. Further research with more individuals and modified methods may be needed to confirm the findings of this study.

TABLE OF CONTENTS

LIST OF TABLES

Table Page

LIST OF FIGURES

Figure Page

CHAPTER I

ANALYZING THE EFFECTS OF BODY SIZE ON FROG SWIMMING

Introduction

Quantifying the effects of body size on locomotion has long been a topic of interest in biology (Calder 1984). However, this is a difficult task because these effects are varied and numerous. Within walking, flying, and swimming animals that use appendage movement to generate force needed for locomotion, many variables that affect performance scale with body size such as leg posture, stride frequency and stride length, wing beat frequency as well as the upper body size limit for flight, and the energy cost of travel as well as travel cost relative per unit mass (Calder 1984; Biewener and Patek 2018). Further difficulty arises when considering the fact that body size and the size of traits that affect locomotion do not always scale isometrically (Calder 1984; Pelabon 2014). For example, the upper body limit for flight is directly affected by the unequal scaling of traits with body size. We know that the power necessary to achieve flight has a positive allometric scaling with mass with a scaling exponent of about 1.7, whereas the force output of flight muscles scales negatively with mass at an exponent of 0.067

(Pennycuick 1972; Calder 1984). Allometric scaling relationships can even affect biomaterials (e.g., bone density, tendon, and muscle) within animals (Biewener 2005). If we consider the Achilles tendon in the heel for example, it has been shown that the amount of energy capable of being stored by the tendon scales with body weight positively with an exponent of 1.28 in quadrupedal mammals (Peterson et al. 1984; Biewener 2005).

If we narrow our focus to aquatic locomotion for the purpose of this study, we see many prominent effects of body size and scaling (Biewener and Patek 2018; Clemente and Richards 2013; Webb 1984). Perhaps the most important effect of size is drag. Drag is the resistive force exerted by the fluid on the body and is as such proportional to the density of the fluid, body shape and orientation relative to the fluid flow, the surface area of the animal, and the swimming speed (Biewener and Patek 2018). Unless comparing between two different media, the fluid density is a constant, and thus the non-constant factors affecting drag are surface area, swimming speed, body shape, and body orientation. If we assume an isometric scaling with growth, surface area increases proportionately to volume at a factor of 2/3. Under this assumption, drag force will increase with surface area at roughly the same factor, since larger animals will have larger surface area, they will typically experience higher drag (Biewener and Patek 2018). For a given body size, shape, and orientation, drag also depends on swimming speed. However, there are many scaling factors that change with size that also can impact swimming speed (e.g., muscle force and propulsive surface area). Relatively larger

animals should exert more propulsive force on the due to having larger muscles, since muscle force increases with muscle cross-sectional area (Biewener and Patek 2018; Clemente and Richards 2013; Vogel 2013). Relatively larger animals also typically have a larger propulsive surface (feet, tails, fins, etc.), which increase the propulsive force exerted as well (Nauwelaerts et al. 2005). This theoretical increase in propulsive force would imply that relatively larger animals should also reach higher swimming speeds, which would in turn also produce a higher resistive surface drag, which larger animals would already experience due to size. Thus, there is an intricate relationship between size, swimming speed, and drag resistance. Understanding all these factors can help shed light on whether a larger body size is advantageous for swimming performance in a unique system.

Currently much is known about the functional morphology and performance of anuran swimming (Moen et al. 2013; Moen et al. 2016; Moen 2019; Robovska-Havelkova et al. 2014; Richards 2010; Clemente and Richards 2013; Nauwelaerts et al. 2005; Johansson and Lauder 2004). From a large scale, it has been shown that the evolution of morphology related to increased swimming performance in semi-aquatic species, like increased foot webbing and relatively large leg muscles, can be largely attributed to selective pressures of microhabitat use (Moen et al. 2013; Moen et al. 2016; Moen 2019). Since both above traits should scale with body length as a frog grows, a scaling exponent of 2 for both cross sectional muscle area and foot-webbing would suggest isometric growth. However, having the largest muscles does not imply the

highest force output. Clemente and Richards (2013) suggest the mechanics of muscle shortening can result in a size constraint. Muscles regardless of size also rely on shortening speed as a factor of force output. Force calculations using a robotic frog foot model suggest that larger muscles are limited by the inability to shorten at the optimal one-thirds of maximum shortening velocity (Clemente and Richards 2013). Furthermore, the kinematics and propulsion generation of frog swimming has also been well studied. Studies suggest that swimming kinematics vary between species based heavily on the ecology of those species (Robovska-Havelkova et al. 2014; Richards 2010). Mechanism for propulsion generation has been shown to stay consistent between species and body sizes of anurans however, as frogs display drag-based propulsion (Nauwelaerts et al. 2005, Johansson and Lauder 2004). What is unknown is how ontogenetic allometry affects the swimming performance within a species.

In this study, I analyzed the effects of body size and ontogenetic scaling on swimming performance in *Rana catesbeiana*. Based on previous research we know that anuran evolution is heavily affected by ecology of the animal (Moen et al. 2013; Moen et al. 2016, Moen 2019). To account for this in our understanding of body size evolution, we must consider the specific ecology of an animal when deciding what aspect of performance is most important in defining fitness. I chose to focus on the swimming speed as the main metric of performance because of its implications on anuran fitness. As burst swimmers, frogs utilize a power stroke to escape predators, utilizing peak swimming speed for survival. This puts emphasis on peak speed as a performance metric

over other potential performance metrics such as energy conservation, may be the focus of selection in most species (Moen et al. 2013).

The other variables I chose to isolate and analyze in this study are drag, momentum, and circulation of the vortices generated in a kick. I chose these variables for both their hydrodynamic connection to swimming speed, as well as their potential to change with body size (Biewener and Patek 2018; Clemente and Richards 2013: Nauwelaerts et al 2005). Based on the relationship between drag and surface area, and body volume discussed above, I expect to see an increase in drag based proportional to body size as well as higher drag forces at higher velocities. I chose to extract momentum of the water in the x-direction (parallel to the movement of the frog, Fig.1), as an indicator of force exerted by the animal. It is vital for this research to have an accurate measurement of force output, not just for its role in propulsion, but because it should scale positively with muscle size, unless met with constraint, like the constraint of muscle shortening velocity mentioned above suggested by Clemente and Richards (2013). Previous studies suggest that the direction of force exerted by anuran swimming is primarily unidirectional (Nauwelaerts et al 2005; Johansson and Lauder 2004). This allowed me to focus on the x-component of momentum, assuming the y- and z-components are negligible (Fig. 1). Finally, I analyzed the produced vortices, because the rotational momentum of the water acted upon by the foot is ultimatel responsible for the thrust generated on the animal (Nauwelaerts et al. 2005; Drucker and Lauder 2000).

Materials and Methods

Animal collection and housing

I collected individuals of *Rana catesbeiana* from wetland sites at Red Slough Wildlife Management Area (33.72171 N, -094.64198 W) and Little River Wildlife Refuge (33.953333 N, -094.7027667 W) in southeastern Oklahoma on 23–24 April 2020. Animals were collected by hand from bodies of water throughout the sites. I captured 22 individuals (12 males and 10 females) with a size range of 65–180mm in snout-to-vent length (SVL).

Animals were housed individually in 37-liter aquariums with moss substrate and water dishes large enough for each frog to submerge itself. I monitored temperature daily to ensure conditions (20-22º C) remained consistent with previous studies and to avoid poor performance due to stress or poor health (Richards 2010). Individuals were fed crickets three times a week. All work with animals was done in accordance with Oklahoma State University ethics protocol ACUP AS-16-14.

Swimming Trials

I recorded four swimming trials for each individual in a 1.22m x .46 m x .61 m aquarium filled to a depth of 10cm (most frogs) or 20 cm (the two largest individuals) with water temperature varying very little (20±1°C). 20° C has been shown to be sufficient for peak performance in ranid frogs (Navas et al. 1999, Nauwelaerts et al. 2005). I mounted two Edgertronic high-speed cameras (SC1, Sanstreak Corp., San Jose,

CA, USA) above the tank (Fig. 1). One camera was fitted with an infrared filter in order to record the reflected infrared light from the suspended particles (see PIV methods below). The other recorded in ambient light and was used for kinematic data. Both cameras were focused on the singular combined laser plane created by the two, level lasers (see PIV methods below). Both cameras recorded 200 frames per second (fps) and with a shutter speed of 1/210 s, which provided a minimum of 66 frames per video across all the trials selected for analysis (maximum of 161 frames). Higher speeds (250 fps, 500 fps) were tested in accordance with previous digital particle image velocimetry studies of frog swimming (PIV, see methods below), however particle displacement in my recordings was found to be insufficient for PIV (Nauwelaerts et al. 2005; Drucker and Lauder 2000). This could be attributed to differences in methods such as camera resolution, particle size, or interrogation area. Burst swimming was induced by releasing the frogs in the tank at the center of the camera's field of view. Most animals swam upon release, but for animals that remained stationary, I made a loud noise or sudden movement above the animal to elicit a reaction (Moen et al. 2013). Contact was never made with the animal to avoid disturbing the water either on the surface or behind the animals, as any ambient movement would appear in PIV analysis. After recording, I trimmed videos to include only one power stroke and recovery period, defined as the simultaneous motion of both legs from retracted to full leg extension (power stroke) and then returning to the retracted position (recovery; Peters et al. 1996; Richards 2010).

Following previous studies, I held trials multiple times with each individual, aiming to capture a minimum of four recordings that showed a straight and complete stroke (Robovska-Havelkova et al. 2014). While we recorded 4 videos per individuals, note that the quality of the videos, assessed during post processing, led to less than 4 per individual being used. Swimming trials were held daily to ensure I obtained the above target number of usable recordings despite the difficult nature of obtaining recordings. Capturing straight and synchronous kicks, both within the field of view of 473 x 378mm and the thin 5mm laser plane, required many attempts (Stamhuis and Nauwelaerts 2005). Also, these trials were completed every day to avoid the conditioning of wild-caught animals to handling and the lab environment. However, time spent in captivity has been shown to not significantly change performance in a previous jumping study (Zug 1985). Finally, I only included trials where the frogs swam below the surface because surface swimming has different physical characteristics due to surface tension, as well as wave production (Biewener and Patek 2018). In total 53 trial videos were recorded from 18 individuals.

Euthanasia and preservation

Euthanasia of individuals was achieved through administration of benzocaine. This was done by immersing the animal in a mixture of water and benzocaine in a sealed container and allowing the animal to absorb the anesthetic through the skin. After 5 minutes, or until the animal was unable to right itself, I checked for a pulse. If a pulse was detected, the animal was replaced into the bath for another 5 minutes. For larger animals (in this case larger than 120 mm SVL), I injected 5% MS-222 solution directly to the heart.

Once euthanized, the animals were then posed and fixed. Posing was done by extending the animal's legs to full extension and tucking the forelimbs tightly into the abdomen. This position was chosen to mimic the natural position of the glide phase in swimming, as fixed specimens were later used for acquiring drag force measurements (Richards 2010). Posed individuals were placed in a container and submerged with a 10% by volume formalin solution for 3 days. After fixing, the formalin was rinsed away with running water, and the individual was placed in a water bath. This was repeated once a day for 3 days to ensure no formalin remained in the specimen. I then moved the fixed individual into 70% by volume ethanol for storage. All euthanasia techniques for this study were done in accordance with Oklahoma State University ethics protocol, ACUP AS-16-14.

Velocity data and Digital Particle Image Velocimetry (PIV)

First, because I lost data linking frog video IDs to specimen numbers after euthanasia the SVL measurements and drag force data taken from specimens post-mortem could not be applied to recordings from swim trials. To account for the missing SVL data, I measured frog SVL from swimming videos in ImageJ (ver 1.42, Rasband 1997). This was done by first calibrating the image using an image of known distance, then using the measuring tool to measure SVL. To reduce measurement error, SVL was measured from three recordings and then averaged.

I began data collection by first calibrating the cameras using a still frame image recorded from the experimental set up before trials began. In the image a 5 mm calibration plate was placed into the center of the field of view. A calibration factor of 2.7 pixels/mm was determined and applied to all videos. All recordings were filmed with the same cameras, from the same distance, using the same settings listed above. I extracted swimming speed of each trial recording by tracking the displacement of the snout of each animal frame by frame using the point measurement tool in ImageJ (ver 1.42, Rasband 1997). After each video was tracked, the digitization error in the data was smoothed using a quintic spline interpolation in R (version 4.0.3; R core team 2020; Ramsay 2020), taking derivatives to obtain instantaneous swimming speed. Based on these results many trials showed peak swimming well below previously reported peak swimming speed and were thrown out from analysis (Richards 2010, Nauwelaerts et al. 2001)

PIV is a non-intrusive 2-D or 3-D flow visualization technique that maps flow patterns of moving water by shining a laser sheet through the water and having it reflected into a camera by neutrally buoyant tracer particles. The recorded videos can then be used to preform cross-correlation of image pairs (subsequent frames) which estimates particle motion patterns within small windows, known as interrogation areas. This estimation of particle movement is mapped as a velocity vector field displaying the estimated direction and magnitude of fluid velocity. (Drucker and Lauder 2000, Johansson and Lauder 2004, Stamhuis and Naulewaerts et al. 2005)

I first seeded the aquarium with 10µm reflective particles with a specific gravity of .05. Using two continuous infrared lasers, (wavelength = 808 nm, power= 2.5 W), I projected horizontal laser sheets that were 5 mm thick x 18 cm wide at the region of interest (the width of the sheet varied as the projection was conical) into the aquarium. Using these two laser sheets, one directed behind the animal, and one orthogonally directed to its side, I created a single combined sheet (Fig 1.), which helped to reduce any shadows caused by the animal during trials.

I analyzed PIV recordings with the software DaVis (v.8.4, LaVision Inc. Ypsilanti, MI, USA). DaVis estimates particle displacement using a multipass cross-correlation of image pairs (in this case, consecutive video frames; Ford et al. 2019). The calculated displacement when calibrated with a known distance (a 5 mm calibration plate as described earlier) and a known period (the frame rate of the recording) results in a vector field of velocity data (Fig. 3). For PIV analyses, I first preprocessed the images

using a subtract time average filter which calculates the Gaussian average intensity of each pixel and subtracts that from the source image. This is primarily used to reduce noise from dark spaces in the video where no or too few particles are visible, as well as bright spots where individual particles are harder to define. Four passes were performed using a spatial resolution of 24 by 24 pixels and a maximum expected displacement of 10 pixels, which was estimated by tracking the distance the tip of the toe traveled. Multiple passes, as well an accurate expected displacement, help sort out and remove possible errors.

Drag force data

Drag force increases directly with size in almost all non-microscopic systems (Biewener and Patek 2018). Here I aimed to understand just how much it increases over the size range of our specimens. Since data collected with preserved specimens could not be directly applied to corresponding videos, we collected drag force data for a few select individuals of varying sizes, chosen by starting with the smallest individual and selecting every 5^{th} SVL from our range. Resulting in drag force collection from 6 individuals with SVLs of 63.2mm, 69.12mm, 75.67mm, 78.07mm, 83.29mm, 88.65mm (Measurements collected from preserved specimen, not digital measurements resulting in discrepancy from swimming recordings). I collected drag force data for each preserved individual at 0.1 m/s intervals from 0.1 m/s to 2 m/s using a motorized belt driven linear actuator capable of traveling up to 2 m (Fig. 2, model X-BLQ-2095, Zaber Technolgies Inc.,

Vancouver, British Columbia, Canada) and 1 mm thick sheet metal S-mount fit with 6 mm linear strain gauges (Lyttle et al. 1999, Omega Engineering Inc., Norwalk, CT, USA). The specimens were attached to the mount with two bolts through the pelvis and abdomen. Two bolts were used to prevent pitching of the specimen unrelated to strain on the bracket. I calibrated the bracket and strain gauge by collecting voltage readings while hanging a series of weights from the mount. Gradually increasing weight intervals were 1-5g increased in intervals of 1g, 10-50g increased in intervals of 5g, 50-200g increased in intervals of 50g, and finally 200-400 g increased in intervals of 100g. I then converted the weight into force in Newtons and acquired a conversion factor 1.2469 V/N from the resulting slope of average voltage over time from each weight over Newtons.

Momentum per Unit Depth

In this study I used momentum of the water displaced by the foot as an indirect indicator of the force exerted by the animal on the water, as force equals time rate of change of momentum per Newton's second law of motion (thus change in momentum for a given time interval will be proportional to the force applied over the same time interval). Momentum can be calculated from the PIV velocity vector field using the following equation (Ford et al. 2019):

$$p(t) = mv = \int\int \rho\vec{U}(x, y, t)\, dx\, dy$$

Here momentum, p, at each frame (time point *t*) was calculated by integrating the two-dimensional velocity vector $\vec{U}$ (varying in x and y) within the region of interest defined

by the terms *dx* and *dy*. Here ρ is the density of water. I calculated these values using custom MATLAB scripts (R2019a, update 5; The Mathworks, Inc., Natick, MA, USA). In order to extract the momentum of the water acted upon by the foot of the animal and not the momentum of the animal itself, I used a dynamic region of interest whose *y*-dimension is equal to the y-dimension of the velocity vector field extracted from PIV analyses, and whose *x*-dimension stayed behind the animal and expanded towards the animal as it accelerated out of frame. This was achieved by first tracking the coordinates of the posterior end of the animal's pelvis and then setting the left most boundary of our region of interest to 500 pixels to the right from the tracked point. This distance was chosen through trial and error and was consistent throughout trials, as it allowed the region of interest to follow the largest animal as closely as possible without including the animal itself throughout the entirety of the stroke (Fig. 4)

Vorticity and Circulation Data

I calculated and extracted the out of plane component of vorticity of each trial from the PIV analyses using DaVis (v.8.4, LaVision Inc. Ypsilanti, MI, USA). I isolated and extracted the peak clockwise and counterclockwise circulation (m^2/s) from the bottom foot of each trial using custom MATLAB scripts that integrated the selected vortices over space. Only one foot was analyzed since it has been shown that vortices produced by frog swimming are typically symmetrical and do not interact with each other (Johansson and Lauder 2004). I divided the trial recordings into time intervals starting at the last motionless frame (at rest just prior to the stroke) and ending at twice the time of

full leg extension. Using full extension of the leg as the midpoint in an analysis allows us to observe and analyze the formation, shedding, and dissipation of the vortices equally. After data collection, I smoothed the values with a quintic spline using custom scripts in R to reduce noise that might occur due to movement of the animal, ambient movement in the water, and any erroneous vectors that may appear in PIV data (Ramsay 2020).

Statistical analysis

For statistical analysis, seven trials from different individuals (SVL ranging from 74–98 mm) were used to test the effect of body size on the variables examined. These trials were chosen as they remained viable through-out all stages of data processing. Only one trial was used per individual to avoid pseudo replication. First, I ran ordinary least squares regressions for swimming speed, momentum, and both clockwise and counterclockwise circulation, individually, over SVL to identify which characteristics were significantly influenced by body size. Next, since swimming speed, our metric of fitness, is connected hydrodynamically to momentum and circulation, (momentum as a predictor for circulation, and circulation as a predictor for swimming speed). For all regressions, assumptions were tested using the Shapiro-Wilks test to test the normality of the residuals (normality reported as W, significance W_p) and homoscedasticity was tested using a Breusch-Pagan test (BP, significance = $BP_{p)}$ (Shapiro and Wilk 1965; Breusch and Pagan 1979). Assumption test values are reported in table 1. Mean, variance, and standard deviation of all variables are reported in table 2. All analyses were run in R (version 4.0.3). Plots were made using R package ggplot2 (Wickham 2016).

Results

I first regressed each variable over SVL. First, I plotted swimming speed as a function of SVL (Fig. 5). My analysis showed no significant effect of SVL on the peak swimming speed of individuals (p-value =0.056, R^2=0.114). SVL also showed no significant relation to momentum in my data set (p-value=0.154, R^2 =0.233; Fig 6). Similarly, neither clockwise nor counterclockwise circulation were significantly related to SVL (CW p-values of 0.330, R^2= 0.027; CCW p-value=0.284, R^2 =0.068; Fig.7).

The regressions of performance variables to each other also showed a similar pattern of non-significance. Momentum showed no significant effect on speed (p-value = 0.107, R^2 = 0.322 (Fig. 8). Clockwise circulation was the only performance factor to show significant effect on swimming speed (p-values = 0.023, R^2 =0.611) (Fig.8). Counterclockwise circulation showed no significant effect for swimming speed (p-value = 0.330, R^2 = -0.018) (Fig. 10)

The resulting curves for drag data show a mostly expected trend where drag force increased with speed and SVL (Fig. 11). The largest individuals' peak drag at 1300 mm/s and 1400 mm/s recorded forces of 4.66 N and 4.89 N. The two mid-range frogs with SVL measurements of 78.07 mm and 75.67 mm produced peak drag force of 3.53 N and 2.66 N at 1500 mm/s. The smallest frogs broke this trend, producing higher drag than the specimen with an SVL of 75.67 mm and roughly the same amount as the specimen with an SVL of 78.07 mm. I suspect this break from the trend was caused by the forelimbs of

the smallest frogs not holding to the body as tightly during fixing, thus increasing the surface area for drag trials. When the two smallest frogs were removed and the remaining force/speed curves were log scaled, the average slope was 1.91. Drag force is proportional to velocity squared, predicting a slope of 2, validating my results. The log-based regression was significant (Fig. 12, p-value= 2.2e-16, R^2 =0.997)

Discussion

In this study, I set out to analyze the effect of allometry on multiple factors to see if the way they scaled with body size influenced swimming performance, to make inferences on how that may affect evolution of body size in frogs. The first step was to define reasonable metrics for performance based on previous knowledge of anuran and bull frog ecology. Since these animals are burst swimmers who primarily use peak swimming speed to escape predators, we can infer that swimming speed is important to survival, and thus fitness (Moen et al. 2013). Then we identified a select number of variables that previous research showed affected swimming speed. These variables were drag, momentum, and circulation (Biewener and Patek 2018, Nauwelaerts et al.2005, Drucker and Lauder 2000). I then analyzed the significant effect between swimming speed, momentum, and circulation using ordinary least squares regressions between all variables.

First my data showed that SVL did not significantly account for changes in any of the analyzed factors. Despite lack of significance the regression slopes were all positive

and less than an isometric slope of 1. If we were to interpret this as a trend, although more data and further analysis would be needed, it might suggest that these factors do scale with body size and exhibit a negative allometry (Calder 1984; Pelabon et al. 2014). However, a limitation of my data set was the failure to obtain velocities that could reasonably be assumed as "peak". Previous studies have shown closely related species with similar ecology and body sizes found in my data set regularly obtain peak swimming speed closer to 2 m/s (Richards 2010, Nauwelaerts et al. 2001). In my data set the highest achieved swimming speed was roughly 1.4 m/s and the average swimming speed across the trials analyzed was roughly 1 m/s. This is important to recognize as the drag forces were not only higher in larger individuals as shown above, but the discrepancy between drag forces at different body sizes increases as the swimming speed increases (Fig. 10). Furthermore, I can see in figure 8, where speed is plotted over momentum, that there is a pattern of frogs on different ends of the size range traveling at similar speeds. In such cases, I see that the larger animal consistently requires a larger peak momentum to achieve a similar speed as a smaller individual. For example, a frog with an SVL of 80.3 mm traveling at 1.29 m/s and a frog with SVL of 98.8 mm traveling at roughly the same speed, 1.26 m/s, produce peak momentum of 2.57 kg·m/s for the smaller frog and a higher momentum of 4.74 kg·m/s for the larger frog. This observed pattern is not inherently profound, in that, in the face of higher drag forces a larger frog would need to exert more force to reach the same speeds. However, I see again that in this discrepancy the difference appears to get larger at higher velocities. This pattern means that if body

size has a significant effect on these factors, it would appear to be most prominent at peak velocities. In future studies, different methods of stimulus (e.g., speakers, light-based stimulus, or gentle touching) should be explored to elicit a full effort escape response from the animal, which could be quantified by recording more trials, implementing a percentile cut-off, and averaging speeds above that percentile.

Another major limitation that may affect the significance of body size in my analyses is the sample size. The limited number of data sets achieved in this study can be mostly attributed to the difficulty of working with live animals paired with the technical requirements for methods like PIV. Multiple trials were discarded due to factors such as the animal swimming above the laser field, diving in and out of focus, and interference from surface waves, many of which became apparent during post processing, and all of which render them unusable in PIV (Nauwelaerts et al. 2005). A larger data set would not only help identify outliers but would also allow for more complex statistical analysis. For example, the simple observations made above, regarding the increasing discrepancy between the momentum needed to achieve similar velocities in different size frogs, could be analyzed using an ANCOVA test, but with so few degrees of freedom that few outliers would render insignificant results.

Overall, further research is still needed to understand how swimming performance is affected by variation in body size. Although my findings did not support a significant effect of body length on the analyzed variables, there were enough limitations to conclude that my findings were most likely inconclusive.

REFERENCES

Astley, H. C. 2016. The Diversity and Evolution of Locomotor Muscle Properties in Anurans. Journal of Experimental Biology 219: 3163-3173

Biewener, A. A. 1989. Scaling Body Support in Mammals: Limb Posture and Muscle Mechanics. Science 245(4913): 45-48

Biewener, A. 2005. Biomechanical Consequences of Scaling. Journal of Experimental Biology. 208: 1665-1676

Biewener, A., S. Patek. 2018. Animal Locomotion. Oxford University Press. Oxford

Breusch, T. S., A. R. Pagan. 1979. A Simple Test for Heteroscedasticity and Random Coefficient Variation. Econometrica. 47(5): 1287–1294

Calder, W. A. I. 1984. Size, Function, and Life History. Harvard University Press, Cambridge, MA.

Cloyed, C. S., J. M. Grady, V. M. Savage, J. C. Uyeda, A. I. Dell. 2021. The Allometry of Locomotion. Ecology. 102(7): e03369

Drucker, E.G., G.V. Lauder. 2000. A Hydrodynamic Analysis of Fish Swimming Speed: Wake Structure and Locomotor Force in Slow and Fast Labriform Swimmers. Journal of Experimental Biology. 203(16): 2379–2393.

Ford, M.P., H.K. Lai., M. Samaee, A. Santhanakrishnan. 2019. Hydrodynamics Of Metachronal Paddling: Effects Of Varying Reynolds Number And Phase Lag. Royal Society of Open Science. 6(10): 191387

Johansson, C.I., G. V. Lauder. 2004. Hydrodynamics Of Surface Swimming In Leopard Frogs (*Rana pipiens*). The Journal of Experimental Biology. 207(22): 3945-395

Lyttle, A.D., B.C. Elliott, B.A. Blanksby, and D.G. Lloyd. 1999. An Instrument For Quantifying The Hydrodynamic Drag Of Swimmers: A Technical Note. Journal of Human Movement Studies. 37: 261-270

Moen, D. S., D. J. Irschick, J.J. Wiens. 2013. Evolutionary Conservatism And Convergence Both Lead To Striking Similarity In Ecology, Morphology, And Performance Across Continents Frogs. Proceedings of the Royal Society B. 280(1773):20132156

Moen, D.S., H, Morlon, and J. J. Wiens. 2016. Testing Convergence Versus History: Convergence Dominates Phenotypic Evolution for Over 150 Million Years in Frogs. Systemic Biology. 65(1):146-160

Moen. D.S. 2019. What Determines the Distinct Morphology of Species with a Particular Ecology? The Roles of Many-to-One Mapping and Trade-offs in the Evolution of Frog Ecomorphology and Performance. The American Naturalist 194(4): E81-E95

Nauwelaerts, S., E.J. Stamhuis, P. Aerts. 2005. Propulsive Force Calculations in Swimming Frogs I. A Momentum-Impulse Approach. Journal of Experimental Biology. 208(8): 1435-1443

Nauwelaerts, S., P. Aerts, K. D'Août. 2001. Speed Modulation in Swimming Frogs. Journal of Motor Behavior. 33(3): 265-272

Navas, C., R. James, J. Wakeling. 1999. An Integrative Study of the Temperature Dependence of Whole Animal and Muscle Performance During Jumping and Swimming in the Frog *Rana temporaria*. Journal of Comparative Physiology B. 169**,** 588–596

Pelabon, C., C. Firmat, G. Bolstad, K. Voje, J. Cassara, A. Le Rouzic. 2014.Evolution of Morphological Allometry. Annals of the New York Academy of Sciences. 1320(1): 58-75

Peters, S. E., L.T. Kamel, D.P, Bashor. 1996. Hopping and Swimming in the Leopard Frog, *Rana pipiens*: I. Step Cycles and Kinematics. Journal of Morphology. 230(1): 1-16.

Peterson, J.A., J.A. Benson, J.G. Morin, M.J. McFall Ngai. 1984. Scaling in Tensile 'Skeletons': Scale-dependent Length of the Achilles Tendon in Mammals. Journal of Zoology London. 202(3): 361-372

Ramsay, J. O., S. Graves, G. Hooker .2020. fda: Functional Data Analysis. R package version 5.1.5.1.

Richards, C. T. 2010. Kinematics and Hydrodynamics Analysis of Swimming Anurans Reveals Striking Inter-Specific Differences in the Mechanism for Producing Thrust. Journal of Experimental Biology. 213(4): 621-634.

Robovska-Havelkova, P., P. Aerts, Z. Rocek, T. Prikryl, A. Fabre, and A. Herrel. 2014. Do All Frogs Swim Alike? The Effect of Ecological Specialization on Swimming Kinematics in Frogs. Journal of Experimental Biology. 217(20): 3637-3644.

R Core Team. 2020. R: A Language and Environment for Statistical Computing (version 4.0.3). Vienna, Austria: R Foundation for Statistical Computing,

Shapiro, S.S., and M.B. Wilk. 1965. An Analysis of Variance Test for Normality (Complete Samples). Biometrika. 52(3–4): 591–611.

Stamhuis, E. J., and S. Nauwelaerts, 2005. Propulsive force calculations in swimming frogs II. Application of a Vortex Ring Model to DPIV Data. Journal of Experimental Biology. 208(8): 1445-1451.

Webb. P.W., and P. T. Kostecki. 1984. The Effect of Size and Swimming Speed on Locomotor Kinematics in Rainbow Trout. Journal of Experimental Biology. 109: 77-95

Wickham, H. 2016. ggplot2: Elegant Graphics for Data Analysis. Springer-Verlag, New York.

Wikelski, M. 2005. Evolution of Body Size in Galapagos Marine Iguanas. Proceedings: Biological Science. 272(1576): 1985-1993

APPENDICES

APPENDIX A: TABLES

Table 1: Results of Shapiro-Wilks test and Bruesch-Pagan test for each regression. These tests were run to make sure there were no significant effects of non-normality or heteroscedasticity. The non-significant p-values show that random effects were insignificant, thus assumptions were met

Regression	Normality(W)	W p-value	Homoscedasticity (BP)	BP p-value
speed/svl	0.90546	0.3653	0.0030709	0.9558
momentum/svl	0.88621	0.2555	0.7666	0.3813
CW/svl	0.95719	0.7943	3.4589	0.06291
CCW/svl	0.86242	0.1591	0.34388	0.5576
speed/momentum	0.88097	0.2308	1.5974	0.2063
speed/CW	0.90381	0.3547	0.12101	0.7279
speed/CCW	0.91697	0.4462	3.048	0.08084

Table 2. Mean, variance, and stand deviation of all collected variables.

Variable	Mean	Variance	Standard Deviation
SVL (mm)	87.58	75.96	8.715
Swimming Speed (m/s)	1.01	0.102	0.318
Peak Momentum (kg·m/s)	3.62	1.55	1.25
Peak CW Circulation (m^2 /s)	-0.051	0.0007	0.0266

APPENDIX B: FIGURES

Figure 1. Coordinate system used for directional orientation of swimming trials.

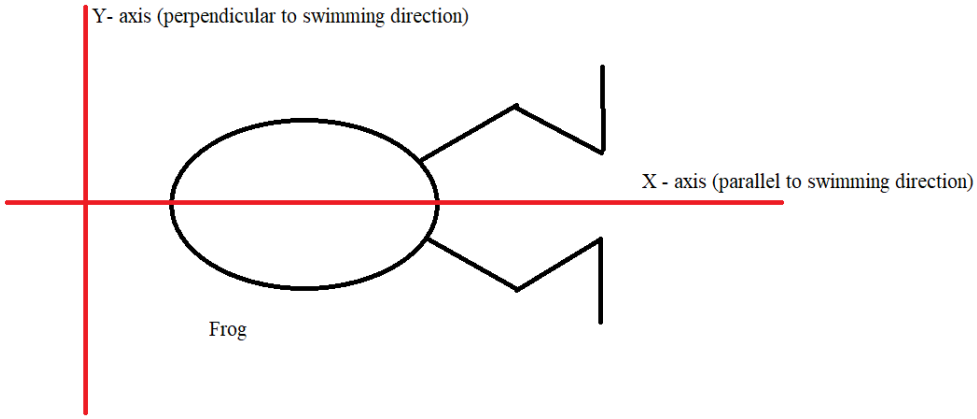

Figure 2. Experimetal setup for swimming trials viewed from the side (top) and above (bottom). Directional coordinates used in analysis correlate with the horizontal and vertical dimensions of the field of view defined in the top view schematic(left). Here the X axis runs along the length of the tank, left to right, and the Y axis runs the width of the tank, top to bottom. Lasers were set up .1m above aquarium floor and .61 m away from the field of view to allow the conical projections to widen to the field of views dimensions.

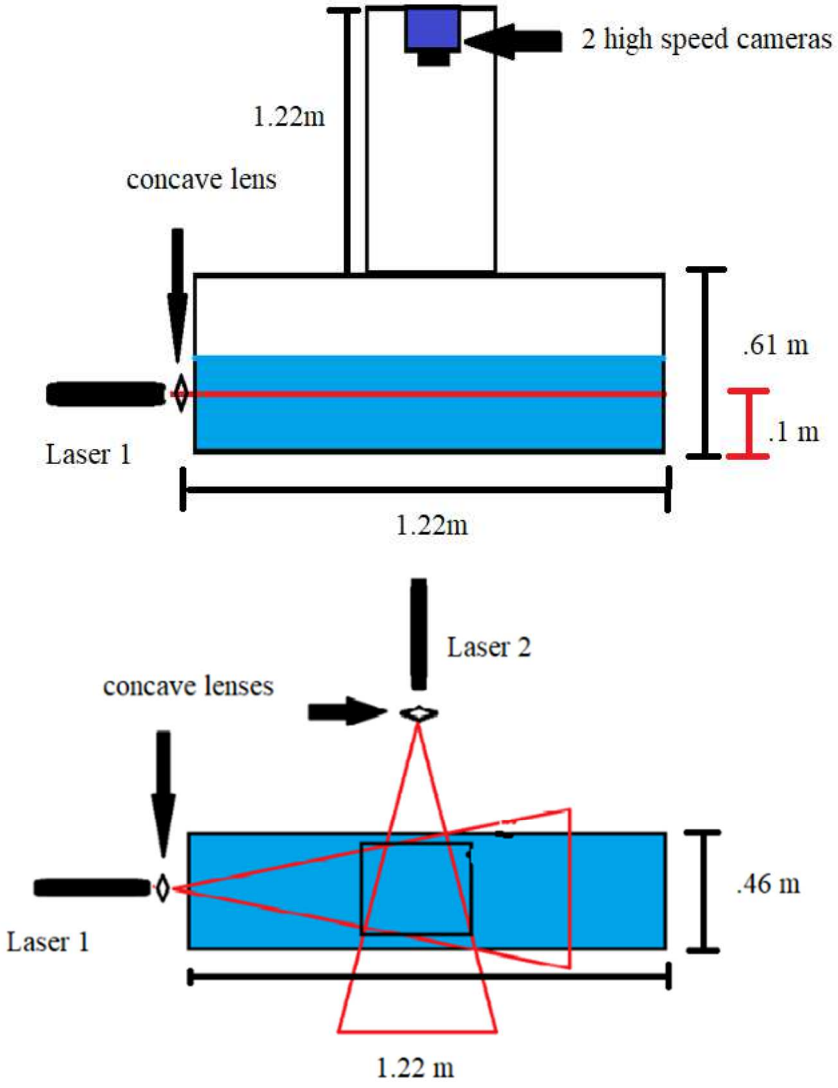

Figure 3. Experimental set up for drag data collection. A 2 m motorized belt-driven linear actuator was mounted atop a 2.43 m aquarium. Preserved specimens were attached to the linear actuator via a mount fitted with a strain gauge.

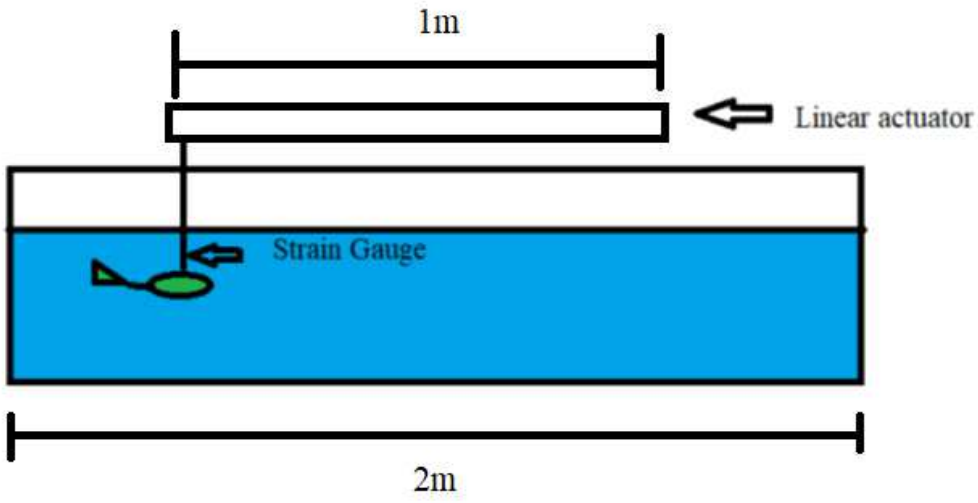

Figure 4. Example of the partial field of view used for momentum calculations. Red polyline indicates that momentum will be calculated from every vector in the region right of the line. This line moves with the animal so that the animal stays on the left of the line and out of the region of interest.

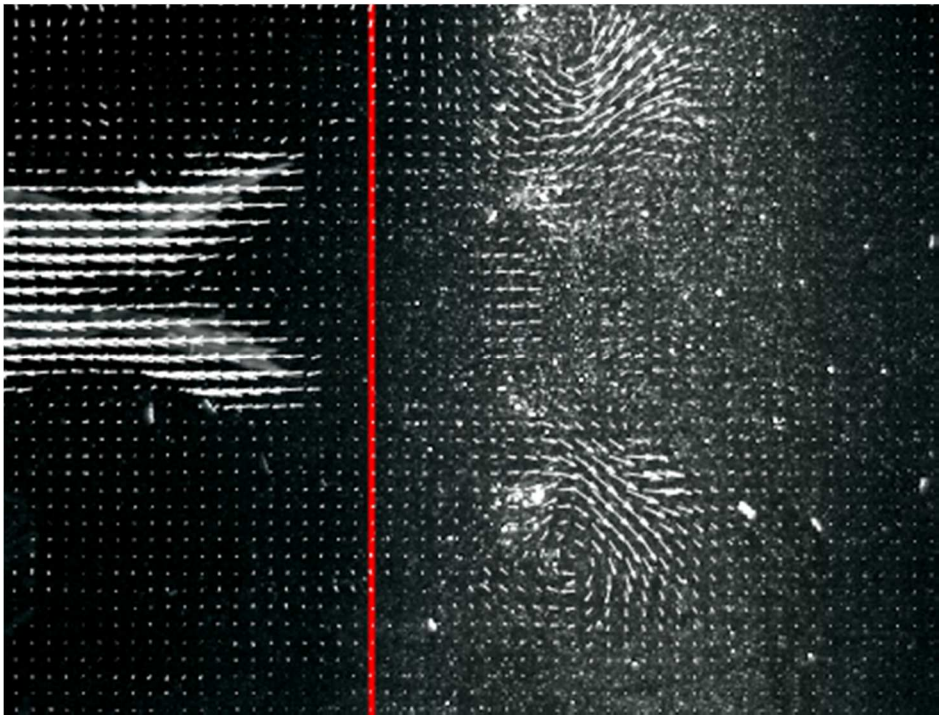

Figure 5. Swimming speed in m/s of each individual plotted over SVL in mm. Linear regressions showed now significant effect on swimming speed achieved (p-value = 0.5614. R^2 = -0.114)

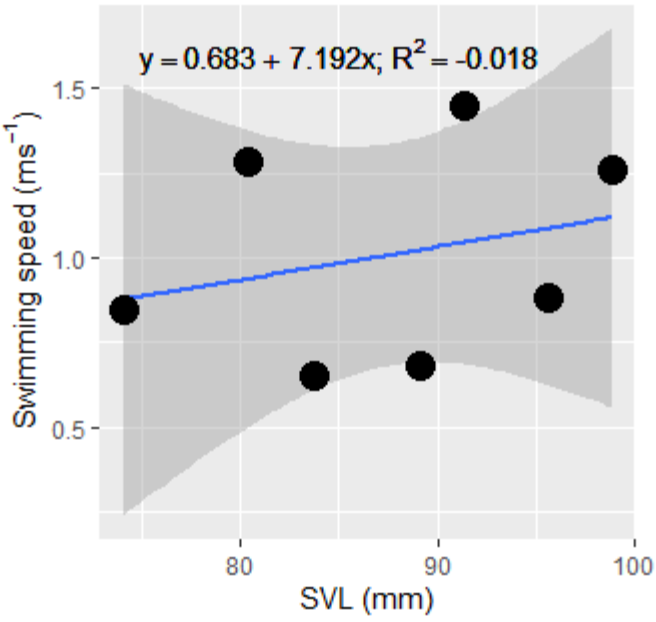

Figure 6. Peak momentum in kg·m s^{-1} plotted over SVL in mm. Linear regression showed no effect of SVL on peak momentum (p-value=0.1537. $R^2 = 0.233$)

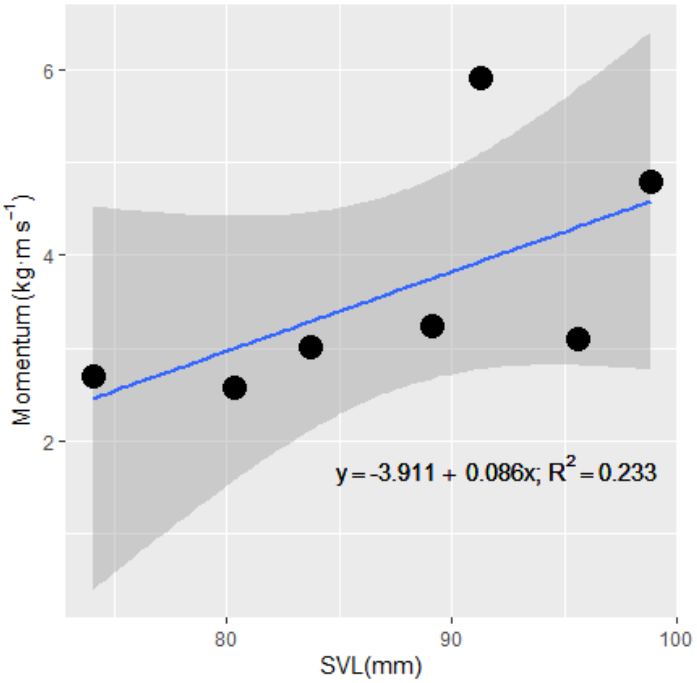

Figure 7. Peak counterclockwise (CCW, top) and clockwise (CW, bottom) circulation in m^2 s^{-1} plotted over SVL. Linear regression showed no significant effect on either counterclockwise circulation (p-value=0.33, R^2= 0.027) or clockwise rotation (p-value=0.2844, R^2=0.068).

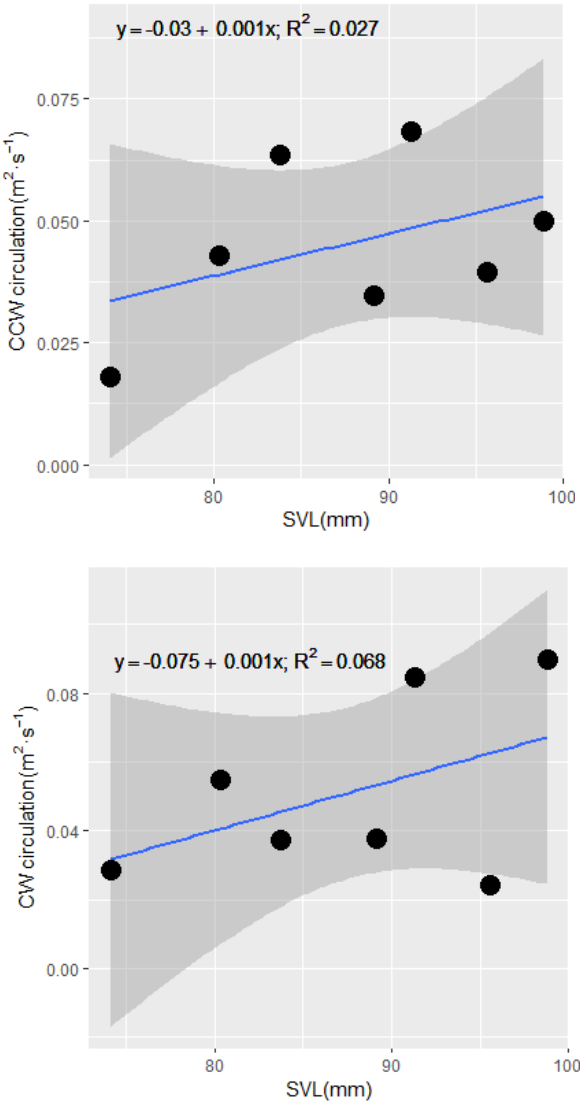

Figure 8. Swimming speed (m s^{-1}) plotted over peak momentum (kg·m s^{-1}) for each trial. Individual's SVL is illustrated via color gradient. The linear regression for Swimming speed over momentum showed no significant effect. (p-value = 0.1068, R^2 = 0.322)

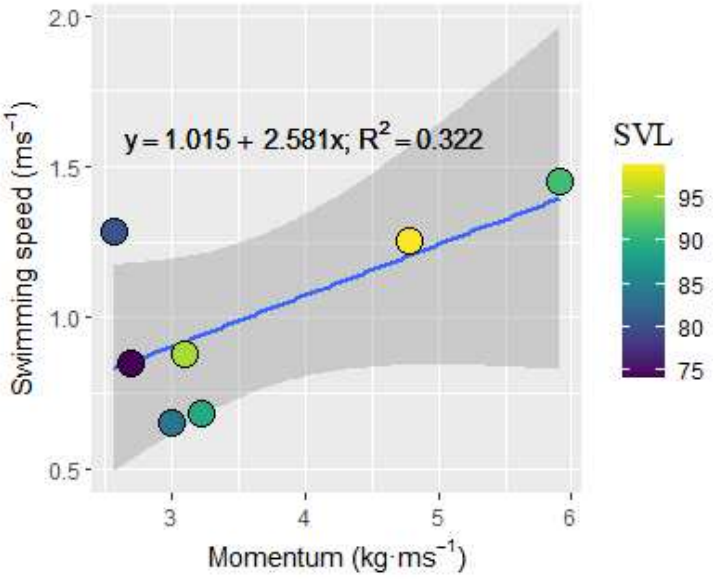

Figure 9. Swimming speed plotted over clockwise circulation showed a significant effect (p-value =.02322, $R^2 = 0.611$).

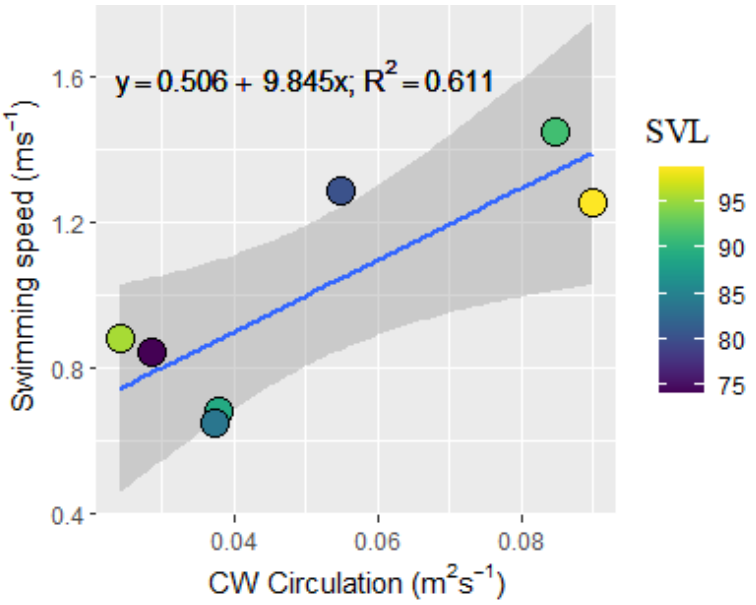

Figure 10. Swimming speed plotted over counterclockwise circulation showed no significant effect (p-value = .33, R^2 = -0.018).

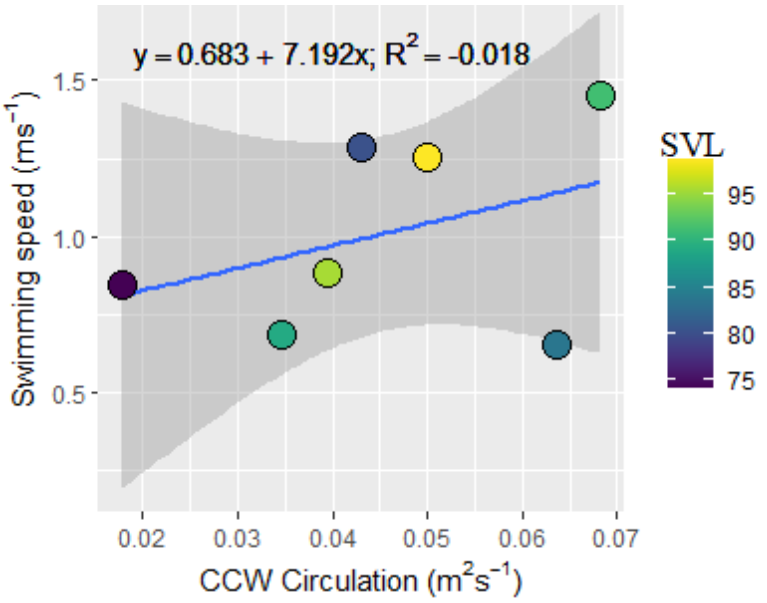

Figure 11. Drag data for a sample of preserved individuals of various sizes. Data points were collected at intervals of 100 mm/s starting at 200 mm/s and ending at 1500 mm/s.

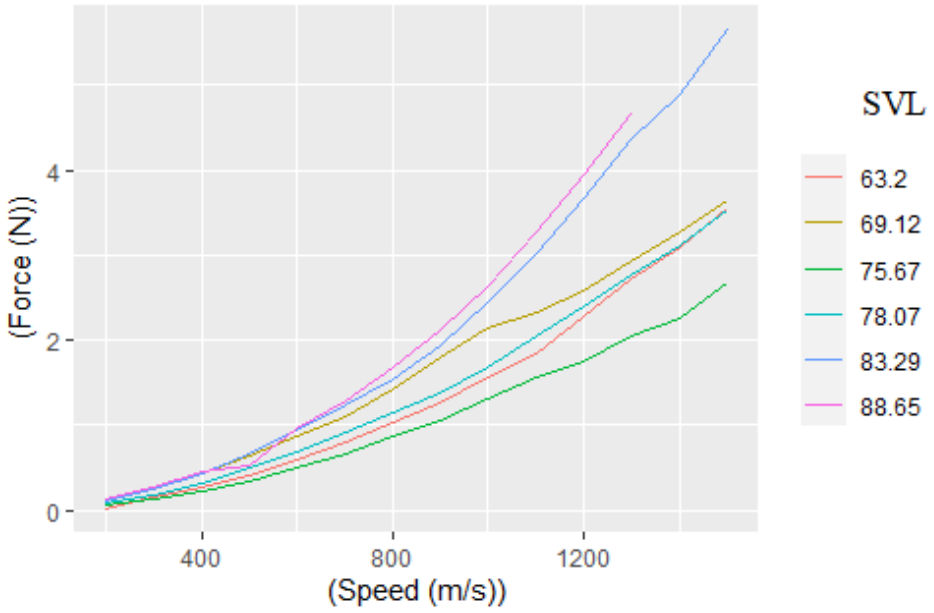

Figure 12. A log scaled regression of drag force over speed. After removing the two individuals that appeared erroneous do to posturing, the average slope is 1.91, where expected scaling of drag force to speed is 2. This regression was significant (p-value = 2.2 $x10^{-16}$, R^2 =0.99)

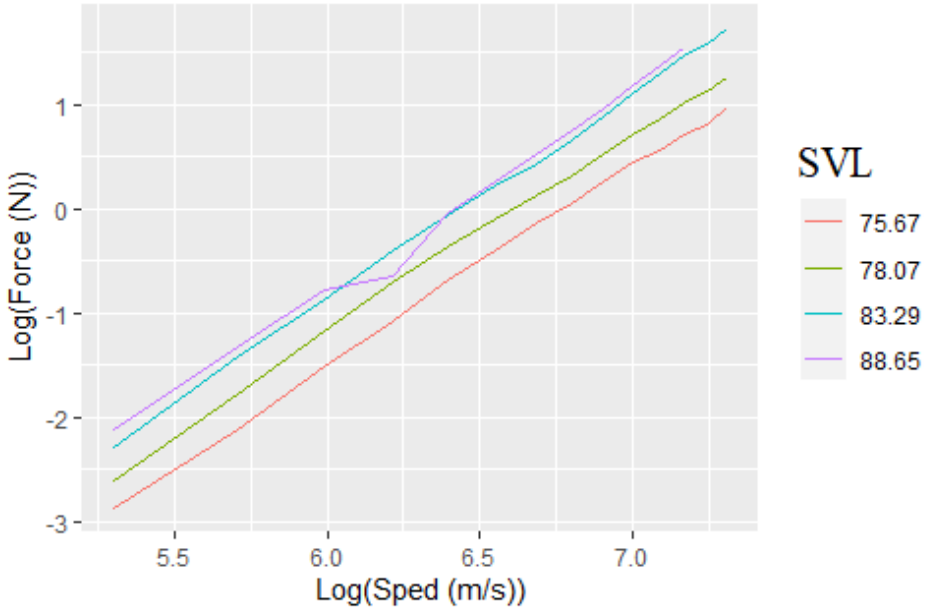

VITA

JACK ROBERT SPICER

Candidate for the Degree of

Master of Science

Thesis: ANALYZING THE EFFECTS OF BODY SIZE ON FROG SWIMMING

Major Field: INTEGRATIVE BIOLOGY

Biographical:

Education:

Completed the requirements for the Master of Science in Integrative Biology at Oklahoma State University, Stillwater, Oklahoma in July 2021.

Completed the requirements for the Bachelor of Science in Zoology at Oklahoma State University, Stillwater, Oklahoma in July 2018